Reversible magnetization of fine-grained high-T_c superconductors

A. S. Krasil'nikov, L. G. Mamsurova, N. G. Trusevich, and L. G. Shcherbakova

N. N. Semenov Institute of Chemical Physics, Russian Academy of Sciences, 117977 Moscow, Russia

K. K. Pukhov

Institute of General Physics, Russian Academy of Sciences, 117333 Moscow, Russia

(Submitted 16 August 1995)
Zh. Éksp. Teor. Fiz. **109**, 1006–1023 (March 1996)

The quasireversible magnetization curves of fine-grained YBaCuO superconductors with grain diameters commensurate with the London magnetic field penetration depth are investigated theoretically and experimentally. Calculated $M(H)$ curves are obtained for a system of cylindrical type-II superconductors ($\kappa = 100$) having different diameters, which correspond to the size distribution of the grains in a real high T_c superconductor polycrystal. A model which takes into account the interaction of the vortices both with one another and with the fields of the Meissner currents and the image field is used in the calculations. A solution is found by an accurate numerical calculation in the case of a small number of vortices $N \leqslant 7$. A method which assumes exact consideration of the interaction of the vortices within the first two coordination spheres and the use of a continuum approximation for the remaining vortices is used for the range of fields $H_{c1} \ll H \ll H_{c2}$. It is shown that the calculated plots of $M(H)$ for type-II superconductors (with consideration of the boundary effects and the size spread) faithfully describe the experimental quasireversible magnetization curves for fine-grained YBaCuO superconductors at $T \geqslant 78$ K not only qualitatively, but also quantitatively. This makes it possible to reveal and account for the peculiarities in the behavior of $M(H)$ caused by the commensurate nature of the linear dimensions of the superconductor and the London penetration depth and to draw a conclusion regarding the degree of correspondence between the magnetic properties of high-T_c superconductors and the properties of conventional type-II superconductors. © *1996 American Institute of Physics.* [S1063-7761(96)02503-9]

1. INTRODUCTION

At high temperatures near T_c, at which the influence of pinning is small, plots of the magnetization $M(H)$ for high-T_c superconductors have a reversible or quasireversible form. The study of the reversible magnetization of high-T_c superconductors is of unquestionable interest, since the behavior of just this curve contains information on fundamental characteristics of the substance being investigated (such as the values of the lower and upper critical fields H_{c1} and H_{c2}, the London magnetic field penetration depth λ, the coherence length ξ, their temperature dependences, etc.). Such information is needed, in particular, in order to understand to what extent the experimental macroscopic magnetic properties of high-T_c superconductors correspond (or do not correspond) to the properties of conventional superconductors.

Investigations of reversible $M(H)$ curves take on special significance when the characteristic linear dimension of the superconductor R is comparable to the London penetration depth λ. As was discovered for classical superconductors,[1,2] the behavior of the $M(H)$ curves of such systems should include features which reflect specific details of the initial shaping of the vortex structure. The specific features exhibited by fine-grained polycrystalline YBaCuO high-T_c superconductors, in which the linear grain dimensions are commensurate with the London penetration depth, were described in 3. In particular, it was shown in Ref. 3 that when the mean linear dimensions of the grains in a high-T_c superconductor decrease to values of the order of 1 μm, the formation fields of both the first and the next seven vortices increase significantly (by more than an order of magnitude) with a resultant considerable shift of the position of the maximum on the $M(H)$ curves toward stronger fields in the high-temperature region ($T \geqslant 80$ K).

The conclusions drawn in Ref. 3 follow from a comparison of experimental $M(H)$ curves with calculated curves obtained using a model which takes into account the interactions of the vortices both with one another and with the surface (i.e., with the Meissner shielding currents and the image field). In this case a polycrystalline, compactly sintered high-T_c superconductor was modeled by a set of long cylinders of isotropic type-II superconductors which are oriented along the applied field H_0 and have a diameter D equal to the mean grain diameter in the sample under consideration. In other words, it was assumed that a stack of grains parallel to H_0 in a compactly sintered sample can play the role of a continuous cylinder from the standpoint of the dynamics of vortex penetration. (The use of the effective parameter λ_{eff} makes it possible to implicitly take into account the real anisotropy of λ in the grains of the polycrystal.)

Employment of this model essentially means that the demagnetizing factor of the grains is neglected. Such an assumption can be fully justified in the cases of close packing of the grains (when the density ρ of the polycrystal is greater than 85% of the single-crystal density) and small values of

 1063-7761/96/030542-10$10.00

$4\pi M$ in comparison with V and H (Refs. 4 and 5). Both of these situations were realized in the fine-grained YBaCuO samples investigated in Ref. 3. This density amounted to 92% of the single-crystal density, and the values of the magnetization did not exceed 2 and 0.3 G in fields of the order of 200 Oe or more at temperatures equal to 85 and 90 K, respectively.

The use of the cylinder model turned out to be productive, since it made it possible not only to calculate the field dependence of the magnetization $M(H)$ for different vortex configurations (with variation of their number from 1 to 7) and different values of the R/λ ratio, but also to obtain both qualitative and semiquantitative agreement between the calculated and experimental curves at $T=85$ and 90 K in fields near the lower critical field.

It was not possible to draw conclusions regarding a more complete quantitative correspondence between the calculated and experimental curves in Ref. 3 due to the lack of a theoretical analysis of the $M(H)$ curve for the same model of cylindrical superconductors with $R\sim\lambda$ over a broader range of fields, as well as the lack of data for evaluating and taking into account the influence of the size distribution of the particles in real polycrystals. According to Ref. 3, the lower critical field H_{c1}, as well as the threshold values of the formation fields for the next vortices, are strongly dependent on the R/λ ratio; therefore, in a polycrystalline sample with moderate values of $R\sim\lambda$, grains of different size will have different magnetizations in the same field H_0.

For this reason, a more complete theoretical analysis of the field dependence of the magnetization $M(H)$ over the broader range of fields $0<H\ll H_{c2}$ for a system of type-II semiconductor cylinders having different diameters, which correspond to the real size distribution of the particles in the fine-grained high-T_c superconductors investigated, would be interesting (and will be conducted herein). Such an analysis will make it possible to compare theoretical curves with the experimental curves for fine-grained polycrystalline YBaCuO superconductors and to draw conclusions regarding the possibility of a quantitative description of the magnetic properties of fine-grained high-T_c superconductors using phenomenological models developed for type-II superconductors, as well as to give an explanation for the experimentally observed peculiarities in the behavior of the reversible magnetization of high-T_c superconductors when the linear dimensions of the individual crystals are comparable in value to the London penetration depth. In order to present a complete picture, some of the results previously obtained in Ref. 3 will be briefly described in the present paper.

2. SAMPLES AND METHODS

The experimental results obtained in the present work for comparison with the calculations were obtained on $YBa_2Cu_3O_{7-\delta}$ samples prepared by the method in Ref. 6 using preliminary mechanical activation of the mixture of the original oxides Y_2O_3, BaO_2, and CuO. The superconducting transition temperature T_c was 92 K, and the degree of rhombic distortion of the crystal cell $(b-a)/(a+b)$ amounted to no less than 0.0084. The data from x-ray powder diffraction analysis attested to the absolute phase purity of the samples.

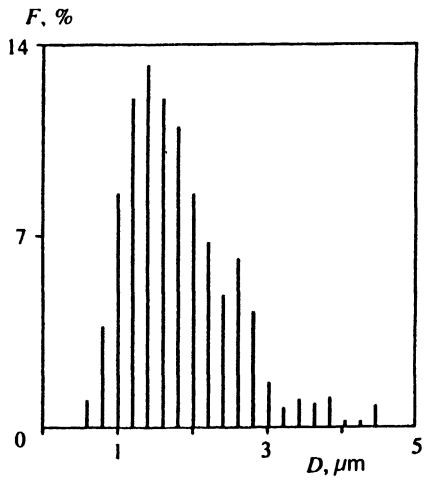

FIG. 1. Histogram of the size distribution of the grains in a fine-grained YBaCuO superconductor.

The density of the samples was no less than 5.83 g/cm^3, which amounts to 92% of the single-crystal density.

Figure 1 presents a histogram of the size distribution of the particles for a typical example of the samples investigated, which was constructed using electron-microscopic data. It is seen that this sample is characterized by a fairly high degree of homogeneity with respect to the grain sizes. (The diameter of a circle having an area equal to the area of the grain image on the photomicrograph is plotted as D in Fig. 1.) Fields with at least 500 grains were selected to construct the histogram. The mean grain diameter in such a sample can range from 1.4 to 1.8 μm, depending on the method used to determine it.

The magnetization measurements were performed by the gravimetric Faraday method on an Oxford Instruments system. The samples were prepared in the form of cylinders with a diameter of about 1 mm and a length of about 8 mm, which allowed us to disregard the demagnetizing factor of the sample.

All the experimental values of the magnetization are given per unit of volume occupied directly by the grains.

3. CALCULATION OF THE FIELD DEPENDENCE OF THE MAGNETIZATION FOR A SUPERCONDUCTING CYLINDER WITH A RADIUS $R\sim\lambda$

Let us consider an isotropic type-II superconductor with $\kappa\gg 1$ in the form of a cylinder located in an external field H_0 (directed along the generatrix of the cylinder) and having a radius R commensurate to the London penetration depth λ.

As reported in Refs. 1, 2, and 7–9, the theoretical description of the magnetic properties of superconductors with a small radius $R\sim\lambda$ has some special features. First, consideration of the interaction of the Abrikosov vortices with the surface, particularly with the Meissner currents and the image field (which is introduced to satisfy the boundary conditions), becomes important in the range of fields $H\geqslant H_{c1}$. The magnetic flux of a vortex filament Φ_v, being a function of the vortex coordinate r_i and the R/λ ratio, is not equal to

the magnetic flux quantum $\Phi_0=\hbar/2c$ and can be considerably smaller. Second, at small fields $H<H_{c1}$, where there are no vortices in the sample, the mean magnetic induction caused by the Meissner currents has a finite value, unlike the negligibly small value in bulk superconductors. When $R\sim\lambda$, this results in a significant decrease in the slope of the initial portion of the $M(H)$ curve from $-1/4\pi$.

In the London approximation, which permits utilization of the technique of superposing currents and fields, the magnetization of a superconductor can be described in the form of a sum of independent contributions:

$$-4\pi M=H_0-(B_L+B_v), \tag{1}$$

where B_L is the mean magnetic induction associated only with the Meissner currents and B_v is the mean magnetic induction created only by the vortex system. More specifically,

$$B_L=\frac{1}{S}\int_S b_L(\mathbf{r})dS, \tag{2}$$

$$B_v=\frac{1}{S}\sum_{i=1}^{N}\Phi_v(\mathbf{r}_i). \tag{3}$$

Here S is the cross-sectional area of the superconductor, N is the total number of vortices in the field H_0, $\mathbf{r}$ is the radius vector in the plane of the cross section, and $b_L(\mathbf{r})$ is the local Meissner field, which satisfies the equation

$$\mathbf{b}_L(\mathbf{r})+\lambda^2\text{curl curl }\mathbf{b}_L(\mathbf{r})=0 \tag{4}$$

with the boundary condition

$$\mathbf{b}_L|_\sigma=\mathbf{H}_0 \tag{5}$$

on the surface σ of the superconductor. Here $\mathbf{b}_L=b_L\mathbf{e}$, where $\mathbf{e}=\mathbf{H}_0/H_0$ is a unit vector parallel to the field.

In the special case of a round cylinder[7,10]

$$b_L=H_0\frac{I_0(r/\lambda)}{I_0(R/\lambda)},\quad B_L=\frac{2I_1(R/\lambda)}{(R/\lambda)I_0(R/\lambda)}H_0, \tag{6}$$

$$\Phi_v(r_i)=\Phi_0\left(1-\frac{I_0(r_i/\lambda)}{I_0(R/\lambda)}\right), \tag{7}$$

where r is the distance from the center of the cylinder in the plane of the cross section, and I_0 and I_1 are Bessel functions of an imaginary argument.

Thus, the reversible magnetization $M(H)$ of a round cylinder (or a system of round cylinders of an identical radius $R\sim\lambda$) is defined as

$$M=-\frac{1}{4\pi}\left[\left(1-\frac{2I_1(R/\lambda)}{(R/\lambda)I_0(R/\lambda)}\right)H_0-\frac{\Phi_0}{\pi R^2}\sum_{i=1}^{N}\times\left(1-\frac{I_0(r_i/\lambda)}{I_0(R/\lambda)}\right)\right] \tag{8}$$

and can be calculated, if the number of vortices and their equilibrium coordinates are known.

Such a problem is solved exactly by minimizing the Gibbs free energy $G^{(N)}$ with respect to the number of vortices and their coordinates. The complete expression for the Gibbs free energy with consideration of the interaction of the vortices with the surface was presented in Refs. 2 and 3.

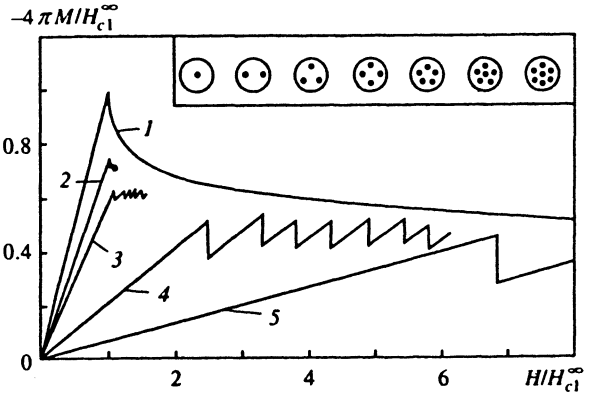

FIG. 2. Calculated dependence of the magnetization $M(H)$ on the magnetic field H for a cylindrical type-II superconductor ($\kappa=100$) and various values of the ratio between the cylinder diameter and the London penetration depth D/λ: ∞ (curve *1*), 14 (curve *2*), 8 (curve *3*), 3 (curve *4*), and 1.5 (curve *5*). Inset: configurations of vortices in a cross section of the cylinder.

Calculated plots of the reversible magnetization for high-T_c superconductors with $\kappa=100$ and different values of the R/λ ratio were obtained, as has been noted, in Ref. 3 for the case of a small number of vortices not exceeding seven (when $R\sim\lambda$, the corresponding range extends over hundreds or more oersteds). Here highly symmetric configurations of the vortices (see the inset in Fig. 2), which have the minimal values $G_{\min}^{(N)}$ and require minimization of the Gibbs free energy with respect to only one parameter, viz., the distance from the vortex to the center of the cylinder, were taken as a base. Figure 2 presents the results obtained in Ref. 3, which reveal how strongly not only the lower critical field H_{c1}, but also the formation fields for each of the ensuing vortices increase as R/λ decreases.[1)] For example, when $R/\lambda=1.5$ (curve *4*), the formation field for the first vortex is 2.5 times greater than the lower critical field H_{c1}^{∞} for an infinite superconductor, and the formation field for the seventh vortex $H^{(7)}$ is 5.8 times greater. This differs radically from the situation realized for the case of an infinite superconductor (curve *1*).

We note that the jumps in the magnetization caused by the penetration of each successive vortex are smoothed in a system of cylinders of different radius. We shall dwell on this point in greater detail later on, since before carrying out the procedure to determine the size distribution of the particles, we must consider the behavior of $M(H)$ for an individual cylinder in higher fields.

As the number of vortices increases, the exact calculations, which call for direct summation using Eq. (3), become a technically difficult task, since they require minimization of the Gibbs free energy with respect to a large number of parameters (all the coordinates of the vortices). For this reason, in the range of fields $H_{c1}\ll H\ll H_{c2}$, where the concept of a vortex density n can be utilized, we employ an approximate calculation method, which contemplates exact consideration of the interaction of the vortices within the first two coordination spheres and the use of a continuum approximation (replacement of summation over the vortex lattice by

integration) for vortices located outside these coordination spheres.

To solve this problem, it is convenient to write the original expression for the Gibbs free energy per unit volume of the superconductor in the form[7]

$$G=\frac{1}{8\pi}\left\{\frac{\Phi_0}{S}\sum_{i=1}^{N} b_v(\mathbf{r}_i)-2H_0B_v-H_0B_L\right\}. \tag{9}$$

Here $b_v(\mathbf{r})$ is the local field of the vortices, which satisfies the equation

$$\mathbf{b}_v(\mathbf{r})+\lambda^2\text{curl curl }\mathbf{b}_v(\mathbf{r})=\Phi_0\mathbf{e}\sum_{i=1}^{N}\delta(\mathbf{r}-\mathbf{r}_i) \tag{10}$$

with the boundary condition

$$\mathbf{b}_v|_\sigma=0. \tag{11}$$

Here $\mathbf{b}_v=b_v\mathbf{e}$.

The field $b_v(\mathbf{r})$ can be represented in the form

$$b_v(\mathbf{r})=\frac{\Phi_0}{2\pi\lambda^2}\sum_{i=1}^{N} K_0(|(\mathbf{r}-\mathbf{r}_i|/\lambda)+b_v'(\mathbf{r}), \tag{12}$$

where $\Phi_0K_0(|(\mathbf{r}-\mathbf{r}_i|/\lambda)/2\pi\lambda^2$ is the field at the point $\mathbf{r}$ created by a single vortex filament with a center having the coordinates $\mathbf{r}_i$, $b_v'(\mathbf{r})$ is the image field, which compensates for the field of the free vortices on the lateral surface of the cylinder σ because of the need to satisfy the boundary condition (11), and K_0 is the modified Bessel function of the second kind of order zero.

Using a known procedure[7] to eliminate the divergence occurring when $|\mathbf{r}-\mathbf{r}_i|\to 0$, we replace the expression

$$\Phi_0K_0(|(\mathbf{r}-\mathbf{r}_i|/\lambda)/2\pi\lambda^2$$

for $i=j$ by H_{c1}^∞, i.e., the lower critical field for an infinite superconductor, and write

$$\sum_{i=1}^{N} b_v(\mathbf{r}_i)=2NH_{c1}^\infty+\frac{\Phi_0}{2\pi\lambda^2}\sum_{i\neq j}^{N} K_0\Big(|(\mathbf{r}_i-\mathbf{r}_j|/\lambda)\Big) -\sum_{i=1}^{N} b_v'(\mathbf{r}_i). \tag{13}$$

When the vortex density is sufficiently large, the last term in (13) can be replaced by an integral:

$$\sum_{i=1}^{N} b_v'(\mathbf{r}_i)\to\int_S b_v'(\mathbf{r})n(\mathbf{r})dS. \tag{14}$$

Such a procedure is justified, since $b_v'(\mathbf{r})$ does not have any singularities in the integration region S.

However, performing a similar operation on the second term in (13), which contains a sum with respect to $i\neq j$, would be incorrect due to the aforementioned divergence of K_0 when $\mathbf{r}_i=\mathbf{r}_j$. Therefore, we write the expression for the second term in the following form:

$$\sum_{i\neq j}^{N} K_0(|\mathbf{r}_i-\mathbf{r}_j|/\lambda)=N[z_1K_0(d_1/\lambda)+z_2K_0(d_2/\lambda)] +\sum_{i=1}^{N} n\int_{S-\delta S}K_0(|\mathbf{r}-\mathbf{r}_i|/\lambda)dS. \tag{15}$$

where z_1 and z_2 are the numbers of vortices in the first and second coordination spheres, respectively, and d_i is the radius of the ith coordination sphere. Here and in the following we assume that the vortex density n does not depend on r.

The meaning of the proposed approximation is as follows. A region of area $\delta S=\pi a^2$ (where $d_2<a<d_3$), within which the interaction between the vortices is taken into account exactly [the first term in (15)], is demarcated around each vortex. The continuum approximation is used for vortices located outside this circle, and, accordingly, the integration region δS must be excluded from the surface integral [the second term in (15)].

Substituting (14) and (15) into (13), we obtain

$$\sum_i b_v(\mathbf{r}_i)=2NH_{c1}^\infty+N\frac{\Phi_0}{2\pi\lambda^2}[z_1K_0(d_1/\lambda) +z_2K_0(d_2/\lambda)]+nSB_v -Nn\frac{\Phi_0}{2\pi\lambda^2}\int_{\delta S}K_0(r/\lambda)dS. \tag{16}$$

Thus, for the density of the Gibbs free energy we have

$$G=\frac{1}{8\pi}\left\{\Phi_0\left[2nH_{c1}^\infty+B_vn+n\frac{\Phi_0}{2\pi\lambda^2}(z_1K_0(d_1/\lambda) +z_2K_0(d_2/\lambda))-\Phi_0n^2\int_0^a\rho K_0(\rho)d\rho\right]-2H_0B_v -H_0B_L\right\}. \tag{17}$$

In going from (9) to (17) we specified the size of the region δS:

$$n\delta S=z+1$$

or

$$\pi\lambda^2a^2n=z+1,$$

where a is the radius (in units of λ) of the circle with an area δS demarcated, and z is the total number of vortices taken into account exactly in the two coordination spheres.

We note that in the limiting case of a bulk superconductor and in fields close to H_{c1}, Eq. (17) transforms into the familiar expression:[12]

$$G^\infty\cong\frac{B}{4\pi}\left[H_{c1}^\infty-H_0+\frac{1}{2}z_1\frac{\Phi_0}{2\pi\lambda^2}K_0(d_1/\lambda)\right].$$

From the condition for the minimum of the Gibbs free energy (17) we find an expression for the magnetic induction and, accordingly, for the magnetization

$$-4\pi M=H_{c1}^\infty-\frac{\Phi_0}{8\pi\lambda^2}L(a,d_1,d_2), \tag{18}$$

where

$$L(a,d_1,d_2)=(z_1+z_2+1)F(a)-z_1[2K_0(d_1/\lambda)+d_1K_1(d_1/\lambda)]-z_2[2K_0(d_2/\lambda)+d_2K_1(d_2/\lambda)], \quad (19)$$

$$F(a)=8\frac{1-aK_1(a)}{a^2}-2K_0(a).$$

For a hexagonal lattice $z_1=z_2=6$, $d_1^2=2/\sqrt{3}n$, $d_2=\sqrt{3}d_1$, and

$$a^2=\frac{z_1+z_2+1}{\pi\lambda^2 n}=\frac{13}{\pi\lambda^2}\frac{\Phi_0}{(H_0+(\Phi_0/\bar{\Phi}_v)4\pi M)}. \quad (20)$$

In (20) we used the following relations:

$$n=B_v/\bar{\Phi}_v, \quad (21)$$

$$B_v=4\pi M+H_0\bar{\Phi}_v/\Phi_0, \quad (22)$$

where

$$\bar{\Phi}_v=[1-B_L/H_0] \quad (23)$$

is the mean magnetic flux of a vortex in the cylinder.

The relations (21)–(23) are valid for a cylindrical superconductor when the vortex density is sufficiently large, and they can easily be derived using a generalization of the known relation[7]

$$\Phi_v=\Phi_0[1-\mathbf{e}\cdot\mathbf{h}(\mathbf{r})],$$

where $\mathbf{h}(\mathbf{r})$ is the field which would be present in the cylinder if there were no vortices in it, to the case of $N\gg 1$.

Before utilizing the formula obtained (18) for the magnetization of a cylindrical type-II superconductor with a radius $R\sim\lambda$ in the range $H_{c1}\ll H\ll H_{c2}$, we must ascertain how well this relation describes the limiting case of a bulk superconductor with $R\gg\lambda$, in which it must transform into Fetter's familiar expression[13]

$$-4\pi M=H_{c1}^{\infty}-\frac{\Phi_0}{8\pi\lambda^2}\times\left(\ln\frac{\lambda^2(H_0-H_{c1}^{\infty})}{\Phi_0}+\ln 4\pi+2-C-A_6\right), \quad (24)$$

where $C=0.5772\ldots$ is Euler's constant, and A_6 is a numerical parameter, which depends on the type of lattice: for a triangular lattice $A_6=0.07968\ldots$.

It can be shown that upon passage to the limiting case of $R\gg\lambda$ in (18), where $B_v=B\gg B_L$, $\Phi_v=\Phi_0$, and $H_{c1}=H_{c1}^{\infty}$, we obtain

$$-4\pi M=H_{c1}^{\infty}-\frac{\Phi_0}{8\pi\lambda^2}\left(\ln\frac{\lambda^2(H_0-H_{c1}^{\infty})}{\Phi_0}+14\ln 2+13\ln(\pi/13)-2C+14\right), \quad (25)$$

which coincides with (24) to within some constant Δ. Moreover, its numerical value

$$\Delta=12\ln 2\pi+A_6-C-13\ln 13+12=0.2127\ldots$$

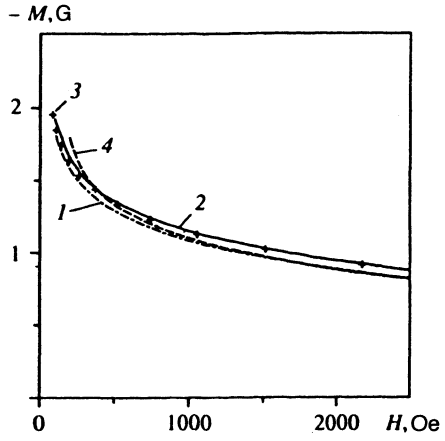

FIG. 3. Field dependence of the magnetization in the range $H\gg H_{c1}$ for a type-II superconductor ($\kappa=100$) of infinite size calculated from Eqs. (18) (curve *1*), (24) (curve *2*), and (26) (curve *3*) and plot for a cylinder with $D/\lambda=3$ calculated from Eq. (18) (curve *4*).

indicates that the sum of the constant terms in Eq. (25) differs from the corresponding sum in Fetter's equation

$$\ln 4\pi+2-C-A_6=3.8741\ldots$$

by only 5.5%.

Calculations show that if the first and second coordination spheres are excluded from the region of exact determination, i.e., if only a circle of radius $a<d_1$ is included in the neighborhood δS in (16), Δ turns out to be equal to -0.4975. This indicates that the small difference between Eq. (25) and Fetter's equation (24) is most likely due to the use of the continuum approximation.

Figure 3 presents the results of the calculations for an infinite superconductor with $R\gg\lambda$ in the range of fields $H_{c1}\ll H\ll H_{c2}$ obtained by three methods: from Eq. (18) (curve *1*), from Fetter's equation (24) (curve *2*), and by the direct numerical method involving minimization of the Gibbs free energy for a triangular vortex lattice (curve *3*):

$$G=\frac{B}{4\pi}\left[H_{c1}^{\infty}-H_0+\frac{3\Phi_0}{2\pi\lambda^2}\sum_{n=1}^{\infty}\sum_{m=0}^{\infty}K_0(d\sqrt{n^2+nm+m^2}/\lambda)\right], \quad (26)$$

where the lattice constant d depends on B as

$$d^2=2\Phi_0/\sqrt{3}B$$

and the first critical field

$$H_{\infty c1}=(\Phi_0/4\pi\lambda^2)(\ln\kappa+0.5). \quad (27)$$

All three curves were calculated for the values $\kappa=100$ and $\lambda=0.47$ μm, which correspond to YBaCuO high-T_c superconductors at high temperatures.

As is seen from Fig. 3, the difference between the plot of (18) for the limiting case of $R\gg\lambda$ and curves *2* and *3* in the range of fields $H<2$ kOe does not exceed 7%.

Such agreement provides some basis to extend the use of Eq. (18) to the case of interest, a cylinder with a finite radius $R \sim \lambda$. Figure 3 presents another plot (curve *4*), which corresponds to the values of λ and κ indicated above (but for the case of $2R = 1.4$ μm) and was calculated from Eq. (18). It turns out that curve *4* for a sample of finite size is essentially identical to curve *1* for an infinite sample by the time $H > 800$ Oe. Calculations show that in fields of about 800 Oe the distance realized between the vortices for the value of R under consideration $d_1 \cong 0.17$ μm, i.e., it can be assumed that the condition $d_1 \ll 2R$ holds at approximately these and higher fields. Hence it follows that Eq. (18) is insensitive to the R/λ ratio at sufficiently high fields, where the distances between the nearest vortices are much smaller than the diameter of the cylinder. Taking into account the closeness of both curve *4* and curve *1* to Fetter's curve, we can conclude that the magnetization of a cylinder with a finite radius $R \sim \lambda$ in the range of fields $H_{c1} \ll H \ll H_{c2}$ can be described directly by using Fetter's equation,[13] which was obtained for an infinite sample (i.e., the region of applicability of Fetter's equation is not restricted by the condition $R \gg \lambda$, which was imposed during its derivation in Ref. 13).

A similar conclusion was previously drawn in Refs. 8 and 9, where the vortex structure in a thin plate of thickness $d \sim \lambda$ was considered in the same range of fields.

The explanation for this effect is probably to be found in Eqs. (21)–(23), which reveal that in a superconductor of small size the difference between the total flux of the entire system of vortices ($n_v \bar{\Phi}_v$) and $n_\infty \Phi_0$ is almost completely canceled by the mean magnetic induction B_L associated with the Meissner current, i.e., $n_\infty \Phi_0 - n_v \bar{\Phi}_v = B_L$, when the vortex density is sufficiently large.

It should also be noted that from the equality between the magnetizations of a finite and an infinite superconductor it must follow that $n_\infty \neq n_v$. Moreover, $n_\infty > n_v$ over the entire range of fields $H \ll H_{c2}$, and the magnitude of this difference depends on R/λ and H_0.

The foregoing treatment makes it possible to obtain the complete plot of the magnetization $M(H)$ (i.e., in fields in the range $0 < H \ll H_{c2}$) for a superconducting cylinder of radius $R \sim \lambda$ and to compare it with experimental $M(H)$ curves observed for fine-grained polycrystalline high-T_c superconductors.

4. COMPARISON OF THEORETICAL AND EXPERIMENTAL MAGNETIZATION CURVES FOR FINE-GRAINED YBaCuO SUPERCONDUCTORS

Figure 4 presents the calculated $M(H)$ curve for a system of superconducting cylinders with the same radius $R = 0.7$ μm, which are characterized by the values $\lambda = 0.47$ μm and $\kappa = 100$ (curve *1*). In segment *AB*, i.e., in the range of fields $0 < H \sim H_{c1}$, the calculation was performed according to Eq. (8) by directly summing the fluxes of the first seven vortices with consideration of the equilibrium configurations (see the inset in Fig. 2). In the range of fields $H \gg H_{c1}$ segment *CD* of the curve is described by Eq. (24), which, as was shown above, is not sensitive to the R/λ ratio.

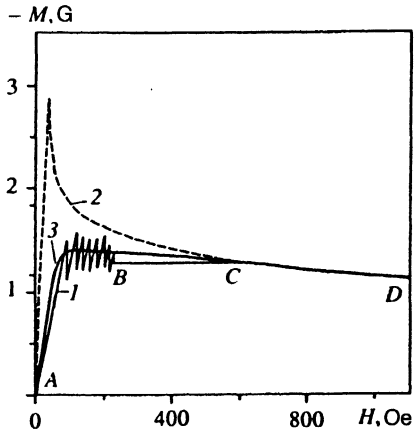

FIG. 4. Calculated field dependence of the magnetization for type-II superconductors ($\kappa = 100$) in the form of a system of cylinders of an identical diameter $D/\lambda = 3$ (curve *1*) and in the form of a system of cylinders of different diameters corresponding to the histogram in Fig. 1 (curve *3*) and for a superconductor of infinite dimensions $D \gg \lambda$ (curve *2*).

For comparison, the calculated $M(H)$ curve for an infinite superconductor with the same values of λ and κ is also given (curve *2*).

It is seen from Fig. 4 that there is an intermediate range of fields (segment *BC*), where the number of vortices $N > 7$, but is still not large enough to use the approximation which is valid in the range $H_{c1} \ll H \ll H_{c2}$. However, as is seen from Fig. 4, in this range of fields the magnetization does not vary too strongly; therefore, we approximate this segment by a constant (straight line *BC*).

Thus, curve *1* completely describes the magnetization of a system of identical cylinders having diameters equal to the mean grain diameter in a real fine-grained YBaCuO superconductor, which we shall use below for comparison.

To take into account the size distribution of the grains realized in the sample under investigation (Fig. 1), the cylinder model used above must be modified in the following manner. We set the diameters of the cylinders equal to different values corresponding to the diameters of the grains in the fine-grained sample under investigation, and we take each of the diameters with a weight corresponding to the histogram of the grain size distribution in Fig. 1.

Calculated curve *3* was constructed in just this manner as the result of numerical averaging of the plots of $M(H)$ for individual cylinders of definite radius, which depend on R/λ. The same values of λ and κ were used.

It is seen, first, that consideration of the size distribution of the particles does, in fact, smooth the jumps in magnetization associated with the penetration of vortices into individual grains. Second, the resultant curve has a gently sloping maximum, which is shifted toward stronger fields in comparison with the $M(H)$ curve for the infinite sample, in agreement with the experimentally observed plots for fine-grained YBaCuO superconductors.

It would be interesting to compare the calculated $M(H)$ curves obtained by the method described above with experimental curves measured at different temperatures in greater detail.

The only variable parameter in the calculations is the

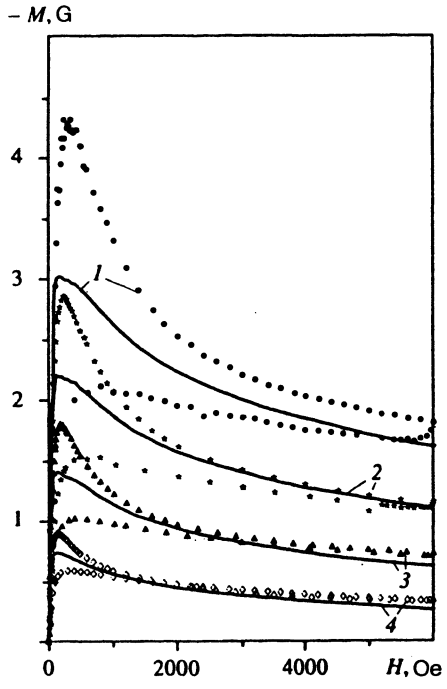

FIG. 5. Field dependence of the magnetization of a fine-grained YBaCuO superconductor at various temperatures $T=78$ (curve *1*), 82 (curve *2*), 85 (curve *3*), and 88 K (curve *4*). The points are experimental, and the solid curves are calculated.

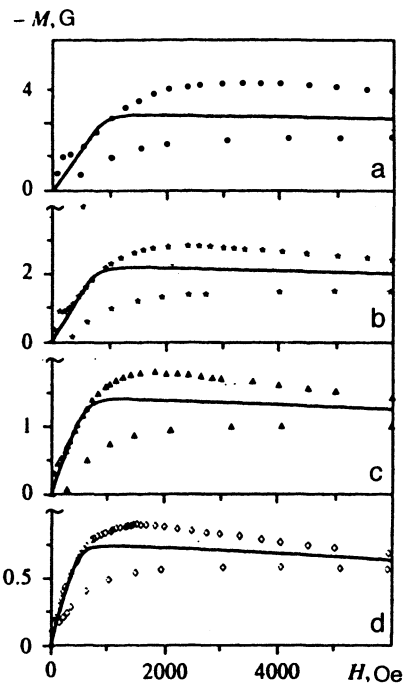

FIG. 6. Initial segment of the magnetization curves of a fine-grained YBaCuO superconductor at various temperatures $T=78$ (a), 82 (b), 85 (c), and 88 K (d). The points are experimental, and the solid curves are calculated.

London penetration depth λ. However, the need to use the same value of λ to describe different portions of a plot of $M(H)$ (which depend differently on it), such as the initial slope and the behavior of the high-field part, imposes strong restrictions on the feasibility of such variation.

When the size distribution of the particles and value of κ are assigned within the model used (κ was set equal to 100 in all the calculations), a comparison of the calculated and experimental curves in the quasilinear segments (which correspond to Meissner shielding of the individual grains) makes it possible to determine the value of λ. However, the existence of a small contribution to the magnetization caused by intergranular currents in very small fields (especially for the compactly sintered samples) introduces a small uncertainty ($\sim 10\%$). The value of λ can be further refined within this 10% interval by maximizing the agreement between the calculated curve and the median of the experimental hysteresis loop in magnetic fields significantly exceeding the field corresponding to the maximum of $M(H)$.

Figures 5 and 6 present the calculated $M(H)$ curves obtained in this manner. It is seen that the calculated curves are in good agreement with the experimental curves and are close to the expected equilibrium curves over the entire range of fields.

However, at temperatures near T_c some disparity begins to appear between the calculated and experimental curves at large fields (Fig. 7a). It should be noted that an influence of the paramagnetic contribution to the resultant magnetization, whose inclusion further exacerbates this disparity, is very likely at these temperatures. (Curve *3* in Fig. 7a is an experimental plot of $M(H)$ obtained at $T=93$ K.) In our opinion, the most likely reason for this disparity is that at 90 K, which is very close to T_c, the distances between the vortex cores cease to be much greater than the coherence length ξ in the range of fields investigated, and, thus, a necessary condition for applicability of the model ceases to hold. In addition, other factors not taken into account in the model are possible in the immediate vicinity of T_c.

At low temperatures, pinning should have a large effect on the experimental curves. This is demonstrated in Fig. 7b, which presents the calculated and experimental curves for $T=20$ K ($\lambda=0.19$ μm) as an example. It is seen that although the calculated curve as a whole is located within the possible range of values, it does not adequately describe the positions of the maximum of $M(H)$ and the median of the experimental hysteresis loop. However, it should be noted that in the case of a strong effect of pinning in a fine-grained sample, the correspondence of the median of the hysteresis loop to the position of the reversible magnetization is not so obvious. Moreover, it is not difficult to show that an influence from another mechanism, which leads to an irreversible magnetization and differs from the one described by the Bean model, is possible in this case. In particular, it can be the mechanism associated with the different positions of the vortices relative to the surface at the moments when the field enters and withdraws. (This question requires a separate investigation.) The existence of such mechanisms should cause the position of the median of the magnetic hysteresis loop not to correspond to a reversible magnetization curve.

Returning to the range of higher temperatures, where the effect of pinning is small, and achieving fully satisfactory agreement on a quantitative level between the calculated and

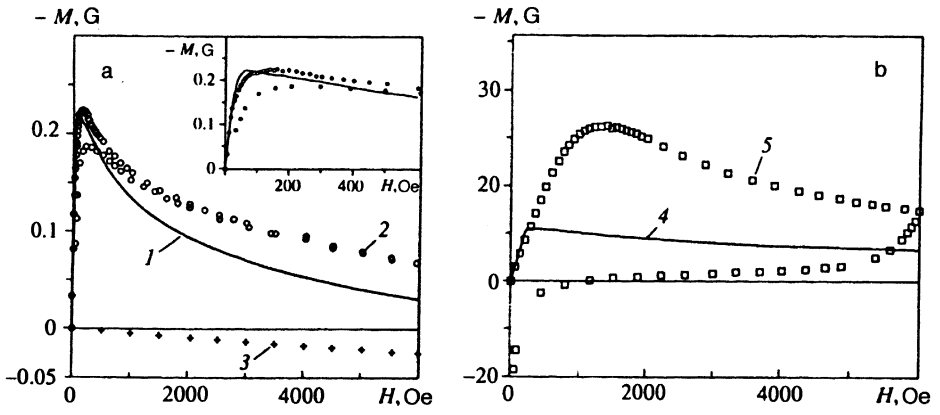

FIG. 7. Field dependence of the magnetization of a fine-grained YBaCuO superconductor at $T=90$ (curves *1* and *2*), 93 (curve *3*), and 20 K (curves *4* and *5*). The points are experimental, and the solid curves are calculated. Inset: initial segment of the magnetization curve at $T=90$ K.

experimental plots of $M(H)$ as a whole, we should discuss the question of the values of the London penetration depth obtained as a result of this comparison.

5. EFFECTIVE VALUES OF THE LONDON PENETRATION DEPTH AND THE LOWER CRITICAL FIELD

Clearly, the values of λ determined from magnetic measurements of $M(H)$ for polycrystalline high-T_c superconductors are essentially effective values, since the individual YBaCuO grains have significant crystallographic anisotropy and $\lambda_{ab} \neq \lambda_c$. However, it was established back in some early studies of high-T_c superconductors[14–17] that in copper-bearing polycrystalline high-T_c superconductors λ_{eff} is determined mainly by the value of the penetration depth of the field H parallel to the c axis of the crystallites, i.e., λ_{ab}. Moreover, since the anisotropy factor for such systems $\gamma=\lambda_c/\lambda_{ab} \geqslant 5$, the value of $\lambda_{ab}/\lambda_{\text{eff}}$ is close to its limiting value of 0.707 in most cases.

Using this relation, we calculated the values of λ_{ab} from the values of the fitting parameter λ_{eff} at all the temperatures investigated. The results are represented by the points in Fig. 8a. For comparison the figure also presents calculated curves for the two-fluid model:

$$\lambda(T)=\lambda(0)[1-(T/T_c)^4]^{-1/2} \tag{28}$$

[where $\lambda(0)=1600$ Å], as well as for the expression

$$\lambda(T)=\lambda(0)[1-(T/T_c)^2]^{-1/2} \tag{29}$$

[where $\lambda(0)=1300$ Å], which, as follows from recent literature data (see, for example, Ref. 18), satisfies the dependence of $\lambda(T)$ in thin films.

As is seen from Fig. 8a, the results obtained from the analysis of the $M(H)$ curves at high temperatures (66–90 K) are described well by both expressions for $\lambda(T)$. A choice in favor of one of them would be possible only if there were sufficiently convincing data in the low-temperature range. Unfortunately, such data cannot be obtained in the present stage of development of the model, which does not take pinning into account.

It can only be noted that the values obtained in the present work, $\lambda_{ab}(0)=1300$ and 1600 Å, are both close to the most frequently used value $\lambda_{ab}(0)=1450$ Å, which characterizes a good YBaCuO single crystal.[19]

In addition, the same data plotted in $\lambda^{-2}(T^2)$ coordinates (Fig. 8b) not only display good correspondence to the law (29), but also fairly definitely attest to the critical temperature $T_c=92$ K for the sample investigated.

In conclusion, it should be noted that the dependence of the threshold fields for the formation of vortices on the grain size noted at the beginning of this paper causes a polycrystalline high-T_c superconductor with a real size distribution of the grains to have a whole range of fields $H_{c1}^{(1)}<H<H_{c1}^{(2)}$, within which vortices first penetrate the largest grains, then the grains with smaller diameters, and finally the smallest grains. The width of this range is clearly determined by the size spread of the grains. Figure 9 presents experimental plots of the dependence of the field at which the magnetiza-

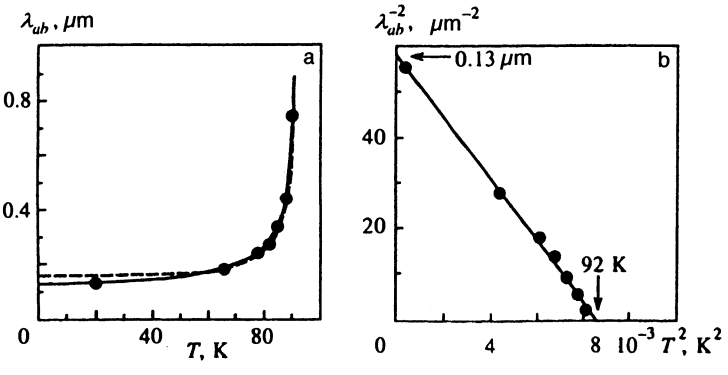

FIG. 8. Dependence of the London penetration depth λ_{ab} on the temperature T (a) and of λ_{ab}^{-2} on T^2 (b) for fine-grained YBaCuO. The points are experimental, the solid curves were calculated from Eq. (29), and the dashed curves were calculated from Eq. (28).

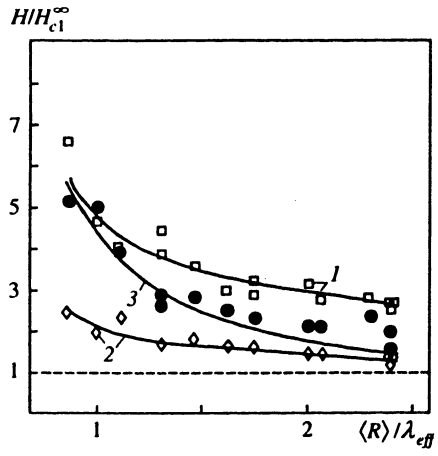

FIG. 9. Fields corresponding to the maximum magnetization (curve *1*) and the first deviation from linearity (curve *2*) as a function of $\langle R\rangle/\lambda_{\rm eff}$ (experiment); calculated dependence of the lower critical field on $\langle R\rangle/\lambda_{\rm eff}$ for a cylindrical type-II superconductor ($\kappa=100$) (solid curve *3*); fields at which there is an average of one vortex per grain (in a plane transverse to the field) — ●.

tion maximum is achieved $H_{\max}$ (curve *1*) and the field corresponding to the first deviation of the $M(H)$ curves from linearity (curve *2*) on the value of $\langle R\rangle/\lambda_{\rm eff}$. (The field at which the difference between the experimental value of the magnetization and the extrapolation of the linear quasireversible segment of the $M(H)$ curve reaches 5% was taken as the field corresponding to the first deviation from linearity.) All the fields were normalized to H_{c1}^{∞}, i.e., the lower critical field for an infinite sample. The experimental points presented were obtained for the same sample at different temperatures in the 70–90 K range. Thus, variation of $\langle R\rangle/\lambda_{\rm eff}$ was achieved only by varying $\lambda_{\rm eff}$, and the influence of the special features of the microstructure of the sample on the results was thereby eliminated. At a sufficiently high temperature $T>70$ K, at which the influence of pinning on the $M(H)$ curve is weak, the field corresponding to the first deviation of $M(H)$ from a linear dependence can be interpreted as the field corresponding to the penetration of vortices into the largest grains. The subsequent increase in the magnetization, as was previously shown, results from the presence of grains into which the field has not yet begun to penetrate. When the fraction of these grains becomes insignificant, the ascent of $M(H)$ ends, and the magnetization reaches its maximum value. Thus, the field corresponding to the first deviation of $M(H)$ from linearity and $H_{\max}$ should be identified with $H_{c1}^{(1)}$ and $H_{c1}^{(2)}$, respectively. (We note that the difference between curves *1* and *2* cannot be attributed to any possible effect of pinning, because this difference does not decrease at all when the temperature rises, i.e., when the value of $\langle R\rangle/\lambda_{\rm eff}$ in Fig. 9 decreases.) If the object studied were a set of grains absolutely identical in size with a radius $R=\langle R\rangle$, matching of the fields corresponding to the first deviation and to achievement of the maximum with $H_{c1}(\langle R\rangle/\lambda_{\rm eff})$ would be expected:[2,20]

$$H_{c1}(R/\lambda)=H_{c1}^{\infty}\frac{\Phi_0}{\Phi_v}\left[1-\frac{K_0(R/\lambda)}{I_0(R/\lambda)[\ln\kappa+0.5]}\right], \qquad (30)$$

where

$$\Phi_v=\Phi_0\left[1-\frac{1}{I_0(R/\lambda)}\right]. \qquad (31)$$

In Fig. 9 this calculated dependence is represented by curve *3*. It is seen that in the most fine-grained sample, for which $\langle R\rangle/\lambda_{\rm eff}\approx 1$, curve *3* is close to curve *1*, and that, conversely, the curve for the more coarse-grained samples with $\langle R\rangle/\lambda_{\rm eff}>2$ corresponds more closely to curve *2*.

We note that the experimental plots of the magnetization $M(H)$ can also be used to calculate the field strengths at which there is an average of one vortex in each grain in the sample (in a plane transverse to the field H_0). This situation corresponds to fields at which the deviation of the magnetization from the linear dependence of $|\Delta M|$ reaches the value

$$4\pi|\Delta M|=B_v=\Phi_v/\pi\langle R\rangle^2,$$

where $\pi\langle R\rangle^2$ is the cross-sectional area of a grain of average size and Φ_v is defined by (31), which corresponds to positioning of the vortex at the center of the cylinder. It is seen that just these field values are very close to curve *3* ($H_{c1}(\langle R\rangle/\lambda_{\rm eff})$), especially in tiny grains. This leads us to believe that the field in which there is an average of one vortex in each grain can be regarded as a certain effective field $H_{c1}^{\rm eff}$ for the polycrystal, which, along with the concepts such as $\mu_{\rm eff}$, $\lambda_{\rm eff}$, and $R_{\rm eff}$ that were introduced and used in Refs. 10, 14–17, and 21, makes it possible to describe the magnetic behavior of a polycrystalline high-T_c superconductor at high temperatures (near T_c) on a quantitative level using phenomenological models developed for type-II superconductors. Moreover, as is seen from the aforesaid, the effective parameters $\lambda_{\rm eff}$ and $H_{c1}^{\rm eff}$ are related in a well-defined manner to the corresponding fundamental characteristics λ_{ab} and H_{c1}, and thus contain the necessary information regarding the substance under investigation.

6. CONCLUSIONS

Thus, a theoretical analysis of the reversible magnetization for cylindrical type-II superconductors with a radius $R\sim\lambda$ has shown that while there are significant changes in the behavior of $M(H)$ at the weak fields $H\sim H_{c1}$ in comparison with a bulk superconductor ($R\gg\lambda$), which are manifested in the variation of the slope of the initial segment, as well as the smoothing of the $M(H)$ curve and displacement of its maximum toward larger fields, the plot of $M(H)$ at the stronger fields $H_{c1}\ll H\ll H_{c2}$ is insensitive to the R/λ ratio.

As the investigations showed, such behavior of the reversible magnetization results from several circumstances. On the one hand, the lower critical fields increase considerably (by more than an order of magnitude) when the linear dimensions of the superconductor decrease to a value $R\sim\lambda$. More importantly, a considerable increase in the applied field is also required for the formation of each successive vortex. This differs radically from the situation observed for superconductors of infinite dimensions ($R\gg\lambda$) and is due to the strong dependence of the vortex flux Φ_v in a superconductor of finite size on the R/λ ratio and on the position of the vortex relative to the surface. On the other hand, when

the vortex concentration increases to such a degree that the distances between the vortices become much smaller than R, the proximity of the surface no longer has an appreciable effect on the magnetization process, since the distortion which the vortex field undergoes near the surface at strong fields is compensated by the mean magnetic induction of the Meissner currents.

A comparison of the calculated $M(H)$ curves obtained (which take into account not only the presence of boundary effects, but also the size spread) with the quasireversible experimental plots for fine-grained high-T_c superconductors in the 78–90 K temperature range reveals that

1) all the aforementioned features of the behavior of the magnetization of type-II superconductors with a finite radius $R \sim \lambda$ are realized for fine-grained YBaCuO superconductors with grain diameters of the order of 1 μm;

2) the experimental $M(H)$ curves for polycrystalline fine-grained YBaCuO superconductors are faithfully described not only qualitatively, but also quantitatively by the curves obtained for isotropic cylindrical type-II superconductors with $\lambda = \lambda_{\text{eff}}$;

3) the more fine-grained the sample, the more closely the position of the maximum of the $M(H)$ curves corresponds to the field at which there is an average of one vortex per grain (in a cross section of the sample transverse to the field). This field is close in magnitude to the value of H_{c1} for grains of average size and can be regarded as a certain effective lower critical field for the polycrystal;

4) the value of the London penetration depth determined for polycrystalline fine-grained YBaCuO high-T_c superconductors from magnetic measurements of $M(H)$ at different temperatures (which are essentially effective values) and the values recalculated for a field parallel to the c axis of the crystallites (λ_{ab}) is described well by known temperature dependences established from measurements by other methods; for example, the value of $\lambda_{ab}(T=0)$ is close to the value $\lambda_{ab}(0) = 1450$ Å, which characterizes a high-quality single crystal.

Thus, the investigations performed in the present work show that the magnetic properties of fine-grained high-T_c superconductors, which reflect fundamental characteristics of the substance, rather than the presence of defects in its crystal structure, fully correspond to the properties of conventional type-II superconductors and can be described not only on a qualitative level, but also on a quantitative level using phenomenological models developed for type-II superconductors.

We thank A. A. Vishnev for prepared the high-quality fine-grained YBaCuO samples.

This work was supported by the Russian Fund for Fundamental Research and the Scientific Council for High-T_c Superconductors and was performed as part of Projects Nos. 95-02-05398 and 93112.

[1)]We recently became aware of the work in Ref. 11, in which similar results were obtained for a disk of small radius.

[1] A. A. Abrikosov, Zh. Éksp. Teor. Fiz. **46**, 1464 (1964) [Sov. Phys. JETP **19**, 988 (1964)].
[2] G. Böbel, Nuovo Cimento **38**, 1740 (1965).
[3] A. S. Krasilnikov, L. G. Mamsurova, N. G. Trusevich *et al.*, Supercond. Sci. Technol. **8**, 1 (1995); A. S. Krasil'nikov, L. G. Mamsurova, N. G. Trusevich *et al.*, Fiz. Nizk. Temp. **21**, 38 (1995) [Low Temp. Phys. **21**, 27 (1995)]; A. S. Krasilnikov, L. G. Mamsurova, K. K. Pukhov *et al.*, Physica C (Amsterdam) **235–240**, 2859 (1994).
[4] U. Yaron, Y. Kornyushin, and I. Felner, Phys. Rev. B **46**, 14 823 (1992).
[5] M. Tinkham, Physica C (Amsterdam) **235–240**, 3 (1994).
[6] A. A. Vishnev, I. V. Kolbanev, L. G. Mamsurova *et al.*, Sverkhprovodimost: Fiz., Khim., Tekh. **7**, 607 (1994) [Supercond., Phys. Chem. Technol. **7**, 587 (1994)].
[7] V. V. Shmidt and G. S. Mkrtchyan, Usp. Fiz. Nauk **112**, 459 (1974) [Sov. Phys. Usp. **17**, 170 (1974)].
[8] V. V. Shmidt, Zh. Éksp. Teor. Fiz. **61**, 398 (1971) [Sov. Phys. JETP **34**, 211 (1972)].
[9] A. I. Rusinov and G. S. Mkrtchyan, Zh. Éksp. Teor. Fiz. **61**, 773 (1971) [Sov. Phys. JETP **34**, 413 (1972)].
[10] J. R. Clem, Physica C (Amsterdam) **153 –155**, 50 (1988).
[11] A. I. Buzdin and J. P. Brison, Phys. Lett. A **196**, 267 (1994).
[12] P. G. de Gennes, *Superconductivity of Metals and Alloys*, W. A. Benjamin, New York–Amsterdam (1966).
[13] A. L. Fetter, Phys. Rev. **147**, 153 (1966).
[14] L. G. Campbell, M. M. Doria, and V. G. Kogan, Phys. Rev. B **38**, 2439 (1988).
[15] V. G. Kogan, M. M. Fang, and S. Mitra, Phys. Rev. B **38**, 11 958 (1988).
[16] S. Mitra, J. H. Cho, W. C. Lee *et al.*, Phys. Rev. B **40**, 2674 (1989).
[17] A. Schilling, F. Hulliger, and H. R. Ott, Physica C (Amsterdam) **168**, 272 (1990).
[18] H. Jiang, T. Yuan, H. How *et al.*, Phys. Rev. B **49**, 9924 (1994).
[19] S. Kamal, D. A. Bonn, N. Goldenfeld *et al.*, Phys. Rev. Lett. **73**, 1845 (1994).
[20] L. G. Mamsurova, K. S. Pigal'skiĭ, V. P. Sakun *et al.*, Sverkhprovodimost: Fiz., Khim., Tekh. **4**, 1919 (1991) [Supercond., Phys. Chem. Technol. **4**, 1829 (1991)].
[21] A. S. Krasilnikov, L. G. Mamsurova, V. P. Oleshko *et al.*, Supercond. Sci. Technol. **7**, 638 (1994).

Translated by P. Shelnitz